Pergamon

International Journal of Plasticity, Vol. 13, No. 4, pp. 291–308, 1997

0749-6419/97 $17.00 + 0.00

PII: S0749-6419(97)00012-0

ANALYSIS OF FAILURE MODES IN IMPULSIVELY LOADED PRE-NOTCHED STEEL PLATES*

R. C. Batra and N. V. Nechitailo

Department of Engineering Science and Mechanics, Virginia Polytechnic Institute and State University, Blacksburg, VA 24061-0219, U.S.A.

(*Received in final revised form* 10 *September* 1996)

Abstract—We analyze transient plane strain thermomechanical deformations of a pre-notched 4340 steel plate impacted by a 4340 steel projectile in the direction of two parallel notches, and study the influence of the impact speed and notch tip radius on the localization of the deformation. The plate configuration is identical to that in Kalthoff's experiments (1987, 1988). There is no failure or fracture criterion included in our work. However, the computed evolution of stress and plastic strain fields strongly suggest that with an increase of impact speed and decrease in notch tip radius, there is a failure mode transition from a tensile crack opening at approximately 70° to the notch ligament to an adiabatic shear band propagating at −5° to −15° to the notch ligament. This is in qualitative agreement with Kalthoff's findings. © 1997 Elsevier Science Ltd

Key words: A. dynamic fracture, B. elastic–viscoplastic material, finite strain, C. finite elements, plate impact.

I. INTRODUCTION

Kalthoff (1987, 1990) and Kalthoff and Winkler (1988) experimentally studied failure modes in double-notched and single-notched polymer and steel plates. Kalthoff showed that with an increase in the impact speed, the failure mode changes from a brittle crack inclined at approximately 70° to an adiabatic shear band inclined at approximately 0° to −15° to the notch ligament. Mason *et al.* (1994) and Zhou *et al.* (1996*a*) experimentally studied failure mode transition in single-notched steel and titanium plates. Ravi-Chandar (1995) conducted similar tests on polycarbonate plates. A goal of these studies was the generation of mode II loading conditions at the notch tip and the corresponding mode of failure. Two critical values V_1 and V_2 for the impact speed were found: no failure was observed for impact speeds below V_1; for impact speeds between V_1 and V_2 a brittle crack propagates at approximately 70° to the notch ligament; for impact speeds exceeding V_2, a shear band propagates in a direction inclined at 0° to −15° to the notch. Kalthoff and Winkler (1988) postulated that the failure mode depends on parameter $V_0/\sqrt{r_0}$, where V_0

*This paper was presented at the symposium, "Dynamic Failure Mode Selection in Solids", organized by A. J. Rosakis, Y. D. S. Rajapakse and R. C. Batra, at Int. Mech. Engg. Congress, San Francisco, 12–17 November 1995.

is the impact speed and r_0 is the radius of the notch tip. Zhou *et al.* (1996*a*) measured peak temperatures of 1427°C near the tip of a shear band in the *C*-300 steel for an impact speed of $42.8\,\mathrm{m\,s^{-1}}$. Shear band speed was found to increase with the impact speed and for a fixed impact speed, the band speed varied as it propagated into the specimen. For an impact speed of $30\,\mathrm{m\,s^{-1}}$, the maximum computed speed of the shear band equalled $1200\,\mathrm{m\,s^{-1}}$. Nechitailo (1995) has reviewed the aforestated works in more detail.

Here we numerically simulate the experimental set-up of Kalthoff (1987) and Kalthoff and Winkler (1988). We assume that both the double-notched plate and the projectile are made of 4340 steel whose thermomechanical deformations are modeled by the Johnson–Cook (1983) relation which accounts for strain-hardening, strain-rate hardening and thermal softening. The main reason for studying a 4340 steel plate is that values of material parameters for the Johnson–Cook model are available in the literature. We investigate the effect of the impact speed of the projectile and the radius of the notch tip on deformations of the material surrounding the notch tip. Our work differs from the numerical work of Zhou *et al.* (1996*b*) who simulated their experimental set-up involving a single-notched plate, applied a prescribed normal velocity field at the impacted surface, and assumed that a material point behaved like a viscous fluid once the effective plastic strain there exceeded the critical value of 0.4. Their prescribed speed seems to be double of what it should be and its drop-off time seems to be too low. Also, when we used their input velocity, the notch surface adjacent to the impacted material moved laterally and struck the other surface of the notch and transferred momentum to it. Zhou *et al.* (1996*b*) applied a large enough force to prevent this. The problem disappeared, at least for moderate impact speeds, when we accounted for the deformations of the projectile and frictional force at the contact surfaces. In our constitutive model, a material point behaves like a compressible ideal fluid once its temperature equals the melting temperature of the material. In the Lagrangian formulation, it is difficult to model an ideal fluid since it can deform severely with a little force. In the results computed thus far, the temperature at any point did not reach the melting temperature of the material, thus the Lagrangian formulation can be used throughout the entire analysis. We do not employ any failure criterion for the notched plate. Deformations of the projectile are not of interest in this work.

II. FORMULATION OF THE PROBLEM

A schematic diagram of the problem studied is shown in Fig. 1. We employ rectangular Cartesian coordinates and the referential description of motion to analyse dynamic plane strain thermomechanical deformations of the bodies. Experimental results indicate that deformations of the plate do not vary much through the thickness; thus the plane strain mode of deformation is a reasonable approximation to the test results. The deformations of the two bodies are governed by the following balance laws of mass, linear momentum, moment of momentum and internal energy.

$$\rho J = \rho_0,\ J = \det \mathbf{F}, \tag{1}$$

$$\rho_0 \dot{\mathbf{V}} = \operatorname{Div} \mathbf{T}, \tag{2}$$

$$\mathbf{T}\mathbf{F}^T = \mathbf{F}\mathbf{T}^T, \tag{3}$$

$$\rho_0 \dot{e} = -\operatorname{Div} \mathbf{Q} + tr(\mathbf{T}\dot{\mathbf{F}}^T). \tag{4}$$

Here ρ is the present mass density of a material particle whose mass density in the reference configuration is ρ_0, $\mathbf{V}$ is its present velocity, a superimposed dot indicates the material time derivative, $\mathbf{T}$ is the first Piola–Kirchhoff stress tensor, e is the specific internal energy, and $\mathbf{Q}$ is the heat flux per unit area in the reference configuration. Here we assume the deformations to be locally adiabatic, thus $\mathbf{Q} \equiv \mathbf{0}$. Also, all of the plastic working rather than 90–95% as proposed by Farren and Taylor (1925) and Sulijoadikusumo and Dillon (1979) is converted into heating.

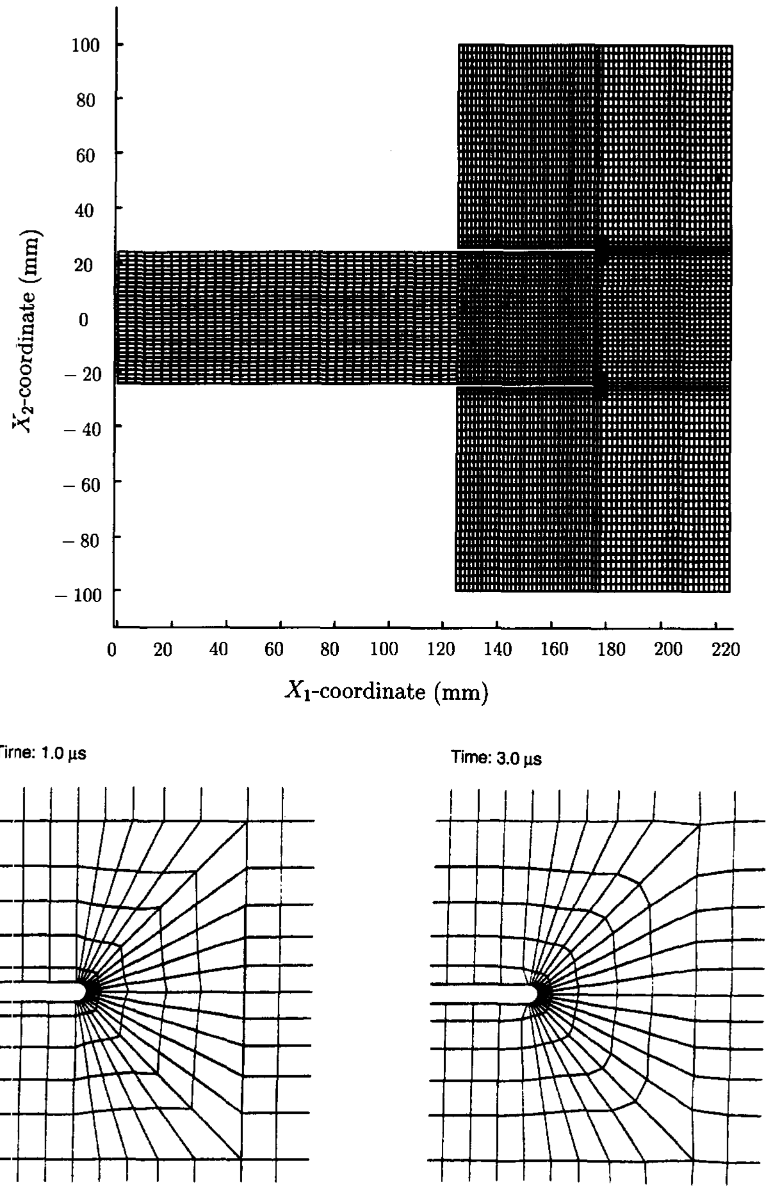

Fig. 1. A schematic diagram of the problem studied, the finite element mesh used, and meshes near the notch-tip generated by the arbitrary Lagrangian–Eulerian method at time $t = 1$ and $3\ \mu s$.

We presume that the projectile and the plate are made of an isotropic elasto–thermo–viscoplastic material and model it by the following constitutive relations.

$$\boldsymbol{\sigma} = -p\mathbf{1} + \mathbf{s}, p = K(\rho/\rho_0 - 1), \ \boldsymbol{\sigma} = J^{-1}\mathbf{T}\mathbf{F}^{\mathrm{T}}, \tag{5}$$

$$\dot{\boldsymbol{\sigma}} = \overset{\triangledown}{\boldsymbol{\sigma}} + \boldsymbol{\sigma}\mathbf{W} - \mathbf{W}\boldsymbol{\sigma}, \ 2\mathbf{W} = \text{grad } \mathbf{v} - (\text{grad } \mathbf{v})^T, \tag{6}$$

$$\overset{\triangledown}{\mathbf{s}} = 2\mu(\overline{\mathbf{D}} - \overline{\mathbf{D}}^p), \ \text{tr } \mathbf{D}^p = 0, \ \overline{\mathbf{D}} = \mathbf{D} - \left(\frac{1}{3}\text{tr } \mathbf{D}\right)\mathbf{1}, \tag{7}$$

$$\dot{e} = c\dot{\theta} - p(\dot{\rho}/\rho^2), \ 2\mathbf{D} = \text{grad } \mathbf{v} + (\text{grad } \mathbf{v})^T. \tag{8}$$

In these equations, K is the bulk modulus, μ is the shear modulus, c is the specific heat, $\boldsymbol{\sigma}$ is the Cauchy stress tensor, p is the hydrostatic pressure, $\mathbf{s}$ is the deviatoric part of the Cauchy stress tensor, $\mathbf{W}$ is the spin tensor, and $\overset{\triangledown}{\boldsymbol{\sigma}}$ is the Jaumann derivative of $\boldsymbol{\sigma}$. Equation (7) is a constitutive relation for a linear hypoelastic material; Truesdell and Noll (1965) have pointed out that it is not invariant with respect to the choice of the objective (frame-indifferent) stress rate. The deviatoric part $\mathbf{D}^p$ of the plastic strain-rate tensor is related to the deviatoric Cauchy stress tensor by

$$\mathbf{D}^p = \Lambda\mathbf{s} \tag{9}$$

where

$$\begin{aligned} &\Lambda = 0 \text{ if either } J_2 < \sigma_m \text{ or } J_2 = \sigma_m \text{ and } s_{ij}\overset{\triangledown}{s}_{ij} \leq 0, \text{ and} \\ &\Lambda > 0 \text{ if } J_2 > \sigma_m, \text{ or } J_2 = \sigma_m \text{ and } s_{ij}\overset{\triangledown}{s}_{ij} > 0. \end{aligned} \tag{10}$$

In the latter case, Λ is a solution of the nonlinear equation

$$J_2 = \sigma_m, \quad J_2 = \left(\frac{3}{2}s_{ij}s_{ij}\right)^{1/2}, \tag{11}$$

$$\sigma_m = (A + B(\varepsilon_p)^n)(1 + C \ \ln(\dot{\varepsilon}_p/\dot{\varepsilon}_0))(1 - T^m), \tag{12}$$

$$\dot{\varepsilon}_p = \left(\frac{2}{3}\text{tr}(\overline{\mathbf{D}}^p\overline{\mathbf{D}}^p)\right)^{1/2}, \quad \varepsilon_p = \int \dot{\varepsilon}_p \text{d}t, \quad T = (\theta - \theta_0)/(\theta_m - \theta_0). \tag{13}$$

Equation (12) is the Johnson–Cook relation (1983) that accounts for the dependence of the flow stress σ_m upon the effective plastic strain ε_p, the effective plastic strain rate $\dot{\varepsilon}_p$ and the temperature θ; A, B, n, C and m are material parameters, θ_m is the melting temperature of the material, θ_0 is the ambient temperature and $\dot{\varepsilon}_0$ is a reference strain rate.

Initially the pre-notched plate is at rest, stress free and at room temperature. The projectile is stress free, at room temperature, is moving with a uniform velocity V_0 in the direction of the notch ligament and just impacts the plate at time $t = 0$.

All bounding surfaces of the projectile and the pre-notched plate except the impacted one are thermally insulated and traction free. At the impacted surface,

$$[\mathbf{v}\cdot\mathbf{n}]=0,\ [\mathbf{n}\cdot\boldsymbol{\sigma}\mathbf{n}]=0,\ \mathbf{f}_t=-(\mathbf{n}\cdot\boldsymbol{\sigma}\mathbf{n})(\mu_s+(\mu_k-\mu_s)e^{-\beta v_{\mathrm{rel}}})\mathbf{t} \tag{14}$$

where $[f]$ denotes the jump in the values of f on the two sides of the impact surface, $\mathbf{n}$ is a unit outward normal to the surface, $\mathbf{f}_t$ is the tangential traction acting along the unit tangent vector $\mathbf{t}$ defined as $\mathbf{v}_{\mathrm{rel}}/v_{\mathrm{rel}}$, values of μ_s, μ_k and β depend upon the roughness of contacting surfaces and $\mathbf{v}_{\mathrm{rel}}$ equals the relative velocity of sliding between the two contacting points. μ_s and μ_k are the static and kinetic coefficients of friction, respectively, and β describes the dependence of the frictional force upon the relative speed of sliding.

III. COMPUTATION AND DISCUSSION OF RESULTS

We assigned the following values to various material parameters for the 4340 steel:

$$\begin{aligned}
&A=792.19\,\mathrm{MPa},\ B=509.51\,\mathrm{MPa},\ C=0.014,\ n=0.26,\ \dot{\varepsilon}_0=10^{-3}\mathrm{s}^{-1}\\
&m=1.03,\ K=157\,\mathrm{GPa},\ \mu=76\,\mathrm{GPa},\ \theta_m=1520^{\circ}\mathrm{C},\\
&c=452\,\mathrm{J\,kg^{-1}{}^{\circ}C^{-1}},\ \rho_0=7850\,\mathrm{kg\,m^{-3}},\ \mu_s=0.18,\ \mu_k=0.05\ \text{and}\ \beta=0.0055.
\end{aligned} \tag{15}$$

These values of material parameters in the Johnson–Cook model are taken from Rajendran's report (1992) and are based on test data at strains, strain rates and temperatures higher than those originally used by Johnson and Cook; however, the maximum strains, strain rates and temperatures involved in these tests are much lower than those likely to occur in a shear band. For large variations in temperature, nearly all of the material parameters in eqn (12) and the shear and bulk moduli are temperature dependent (e.g. see Klepaczko *et al.*, 1987). However, this has not been considered mainly because of the lack of such data.

An approximate solution of the initial-boundary-value problem formulated above is obtained by using the large scale explicit finite element code DYNA2D developed by Whirley *et al.* (1992). It uses quadrilateral elements, one-point integration rule to evaluate various integrals, and an hour-glass control to suppress the spurious modes. It selects the time step adaptively to satisfy the Courant condition and the time step decreases as the mesh gets severely distorted during the development of a shear band. We use the Lagrangian–Eulerian option to rezone the deforming region; however, too frequent remeshing may smooth out the field variables, thereby delaying the localization of the deformation into narrow bands, and lessening the intensity of the plastic strain within these narrow regions. In the results presented below, the deforming region was rezoned after every 195 time steps; numerical experiments gave this to be a good value to use. Magnified meshes near the notch tip at $t=1.0$ and 3.0 μs are exhibited in Fig. 1.

As in all numerical studies involving the localization of plastic deformation into narrow bands, except those using higher-order theories involving one or more material characteristic lengths (e.g. see Needleman, 1988, Batra and Hwang, 1994), results presented below are likely to be mesh dependent. The finite element mesh used here was optimized to minimize errors in the numerical solution at the notch tip and give computed speed of the longitudinal wave nearly equal to the analytical value.

Because of the assumption of locally adiabatic deformations, the balance of internal energy (4) reduces to

$$\rho c \Delta\theta = \mathrm{tr}(\mathbf{s}\mathbf{D}^p)\Delta t. \tag{16}$$

Hence the time step is controlled by the mechanical problem, and the incremental temperature change at a quadrature point can be determined from eqn (16).

The problem is symmetrical about the horizontal centroidal axis; thus deformations of only the upper half of the projectile and the pre-notched plate are analysed even though some of the results presented are for the entire region. We first fix the notch tip radius r_0 at 0.15 mm and study the effect of the impact speed; subsequently we analyse the effect of varying the notch tip radius, and the initial yield stress of the material on deformations of the plate.

IV. EFFECT OF IMPACT SPEED

Figure 2 depicts for $V_0 = 25\,\mathrm{m\,s^{-1}}$ the time history of maximum shear stress, hoop stress and effective plastic strain at four points *a*, *b*, *c* and *d* adjacent to the notch surface and making an angle of $\pm 5°$ and $\pm 70°$ to the notch ligament. The loading wave arrives at the notch tip at about $10\,\mu\mathrm{s}$ after impact which agrees with the analytical estimate since longitudinal wave speed = (Young's modulus/mass density)$^{1/2}$ = 5.02 mm $\mu\mathrm{s}^{-1}$ and the time taken for the wave to arrive at the notch tip = (50/5.02) = 9.96 μs. The effective plastic strain grows rapidly at points *a* and *c* where the maximum shear stress is also higher than that at points *b* and *d*; the locations of these points on the notch surface are indicated in the insert of Fig. 2. However, the maximum tensile hoop stress occurs at point *b*, and the magnitude of the compressive hoop stress at point *d* is more than that of the tensile hoop stress at point *b*. Thus for a material weak in tension, the failure will initiate along a line making an angle of 70° to the notch axis and a material weak in shear will fail along the notch ligament. Once a crack has initiated, new surfaces are created, and the domain of the initial-boundary-value problem will change. We note that the effective plastic strain rate at points *a* and *c* varies with time and its maximum value occurs for $26\,\mu\mathrm{s} \le t \le 33\,\mu\mathrm{s}$ and equals about $8600\,\mathrm{s^{-1}}$.

Figure 3 exhibits contours of maximum shear stress, distribution of hoop stress and contours of effective plastic strain in the vicinity of the notch tip at time $t = 39.2\,\mu\mathrm{s}$ after impact. It is clear that the region with the maximum plastic strain advances straight ahead of the notch tip and the notch tip has also been deformed. The maximum shear stress occurs in a region in front of the notch tip, and the hoop stress is tensile in the region above the notch ligament but compressive in the region below it. For $11\,\mu\mathrm{s} \le t \le 52\,\mu\mathrm{s}$, the hoop stress is compressive in the region where maximum shear stress attains its extreme value. Thus a shear band will propagate essentially along the notch ligament within a region of high maximum shear stress and small compressive stress. A tensile crack, if one initiates owing to high tensile hoop stresses, will propagate along the direction of 70° to the notch axis. Without knowing which material parameter should attain a critical value for the initiation and propagation of a shear band, a shear crack and an opening crack, it is hard to decide which failure mode will initiate first. Kalthoff's experiments suggest that more energy is needed for a shear band and/or a shear crack to initiate and propagate as compared with that for a tensile opening crack.

In Fig. 4 we have plotted the evolution of the horizontal component of velocity at three points on the impacted surface. During the time interval $3\,\mu\mathrm{s} \le t \le 44\,\mu\mathrm{s}$, the magnitude of the horizontal component of velocity at these points is about one-half of the initial speed

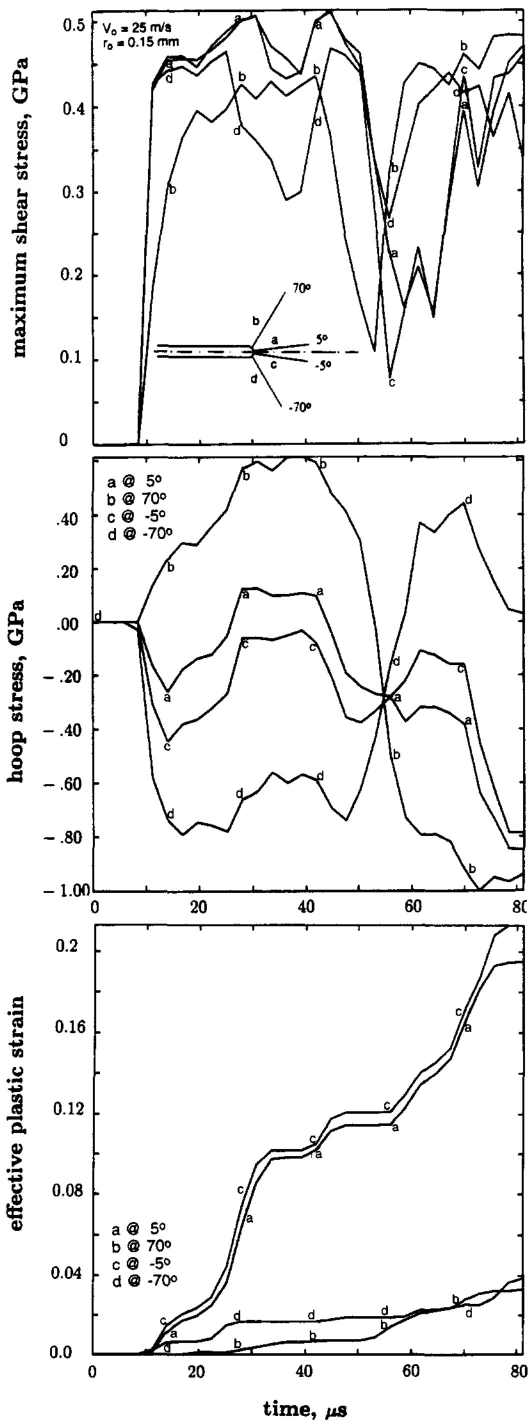

Fig. 2. Time history of maximum shear and hoop stress (GPa), and effective plastic strain, at points adjacent to the notch tip; (a) 5°, (b) −5°, (c) −70° and (d) 70°. Impact speed = 25 m s^{-1}, notch tip radius = 0.15 mm.

of the projectile. At 49.8 μs the tensile wave refected from the free end of the projectile arrives at the impacted surface and separates the two bodies. Subsequently, all surfaces of the pre-notched plate are traction free and its deformations ensue mainly because of kinetic and potential energies imparted to it during the first 49.8 μs of impact. We note

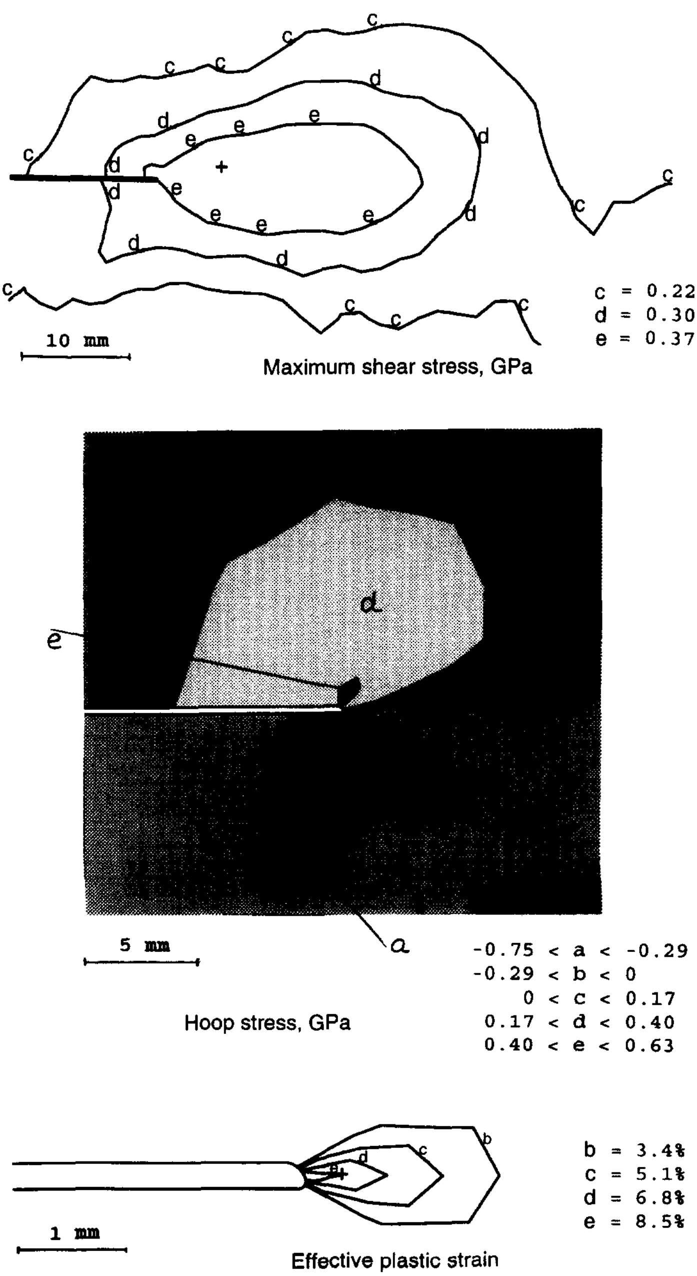

Fig. 3. Contours of maximum shear stress, distribution of hoop stress, and contours of effective plastic strain in the vicinity of the notch tip at $t = 39.2\,\mu s$ after impact. Impact speed = 25 m s^{-1}, notch tip radius = 0.15 mm.

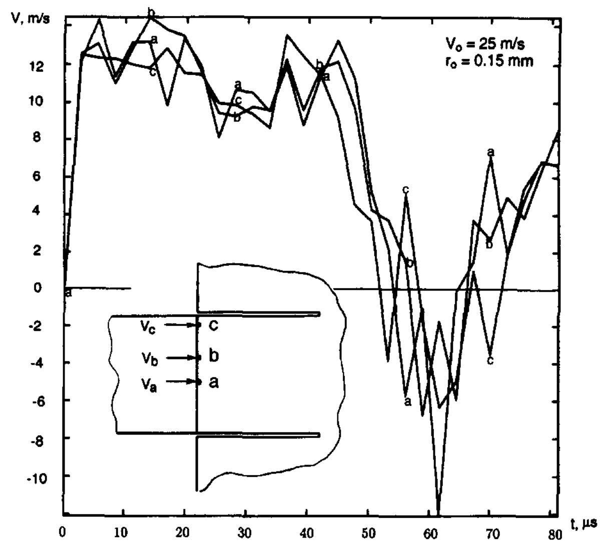

Fig. 4. Time history of horizontal component of velocity at three points on the impacted surface. Impact speed $= 25\,\mathrm{m\,s^{-1}}$, notch tip radius $= 0.15$ mm.

that the rise time of the horizontal velocity of points a, b and c is about 3–5 μs but the drop-off time is close to 10 μs. Also the horizontal component of velocity at points a, b and c does not become zero, simultaneously implying that the reflected wave is not plane, which is to be expected since waves reflected from the lateral boundaries will interact with the wave reflected from the left edge of the projectile.

The shapes of the notch at different times during the deformation process are shown in Fig. 5. The upper and lower surfaces of the notch move owing to shear and compression. Even though the notch tip at $t = 78.4\,\mu$s appears circular, its radius has decreased and its width is no longer uniform. Also, the notch tip during the intervening times is not circular. Numerical simulations conducted for $V_0 = 30\,\mathrm{m\,s^{-1}}$, $35\,\mathrm{m\,s^{-1}}$ and $40\,\mathrm{m\,s^{-1}}$ gave results similar to those obtained for $V_0 = 25\,\mathrm{m\,s^{-1}}$ except that the peak values of the effective plastic strain, hoop stress and the maximum shear stress at points a, b, c and d adjacent to the notch surface were higher than the corresponding values for $V_0 = 25\,\mathrm{m\,s^{-1}}$. Also, more of the plate material was severely deformed as compared with that for $V_0 = 25\,\mathrm{m\,s^{-1}}$. In Fig. 6, we have plotted, at different times, the variation with the impact speed of the effective plastic strain at points b and c on the notch surface. As in Fig. 2, lines joining points b and c to the center of the notch are inclined at 70° and −5° to the notch ligament. It is evident that the effective plastic strain at point b remains small even for $V_o = 50\,\mathrm{m\,s^{-1}}$; however, the tensile hoop stress there is large and increases with an increase in V_0. At point c effective plastic strain is large and maximum shear stress is also significant but the hoop stress is compressive.

At an impact speed of $100\,\mathrm{m\,s^{-1}}$, the plate material between the two notches expanded laterally (owing to Poisson's effect) by an amount large enough to close the gap and impact the upper surface of the notch. In order to avoid closing of the notches we changed the surface of the notch further away from the axis of symmetry of the plate, made the notch width stepped increasing toward the impacted surface. This should not affect deformations of the plate material abutting the notch tip. As shown in Fig. 7(a), the effective plastic strain at points c ($-5°$) and d ($-10°$) grows rapidly, and for $t \geq 56\,\mu s$ is maximum at point d. The evolution of the maximum shear stress at four points on the notch surface located on lines making angles of $\pm 5°$, $-10°$ and $-70°$ with the notch axis, plotted in Fig. 7(b), shows that the maximum shear stress at point d (at $-10°$ to the notch ligament) begins to decrease gradually at $t = 30\,\mu s$. The rate of drop of the maximum

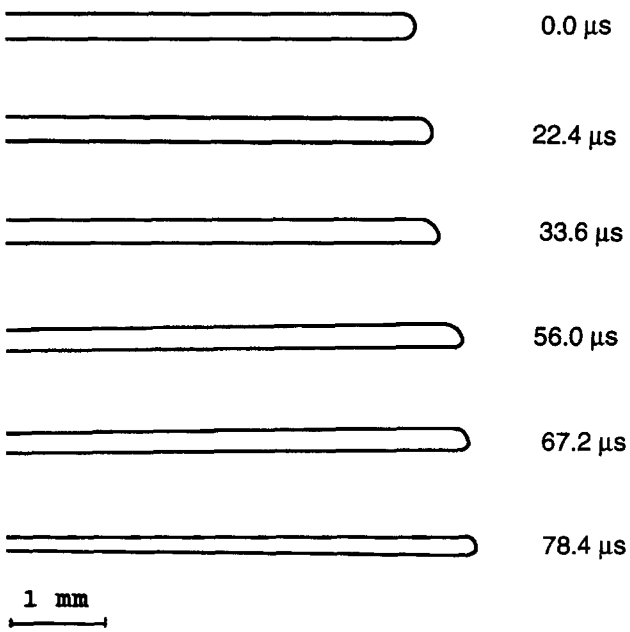

Fig. 5. Shapes of the notch at different times during the deformation process. Impact speed = $25\,m\,s^{-1}$, notch tip radius = 0.15 mm.

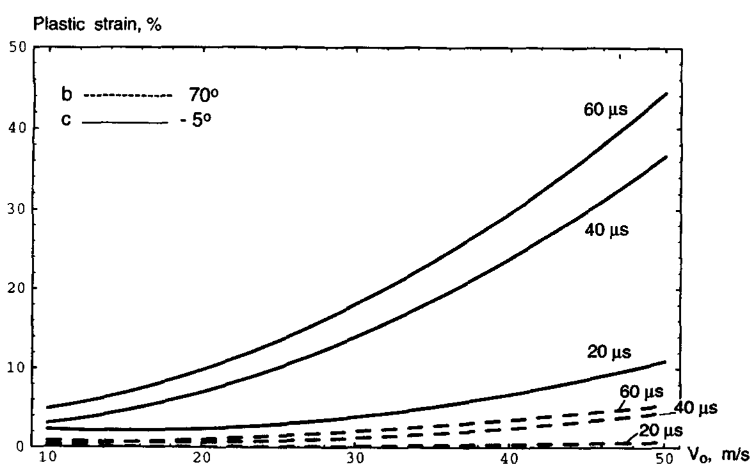

Fig. 6. Dependence on the impact speed of the effective plastic strain at points b and c on the notch surface. Notch tip radius = 0.15 mm.

shear stress accelerates at $t = 65\,\mu s$. One usually associates the drop in the load carrying capacity of a material point with the initiation of a shear band there (Marchand and Duffy, 1988); thus a shear band initiates at point d at about $t = 30\,\mu s$ and intensifies at $t = 65\,\mu s$. Figure 8(a) exhibits the deformed notch tip and contours of the effective plastic strain in the region surrounding the notch tip. It is clear that the notch tip has severely deformed owing to shear; at $t = 53.2\,\mu s$ it has translated in the direction of impact by

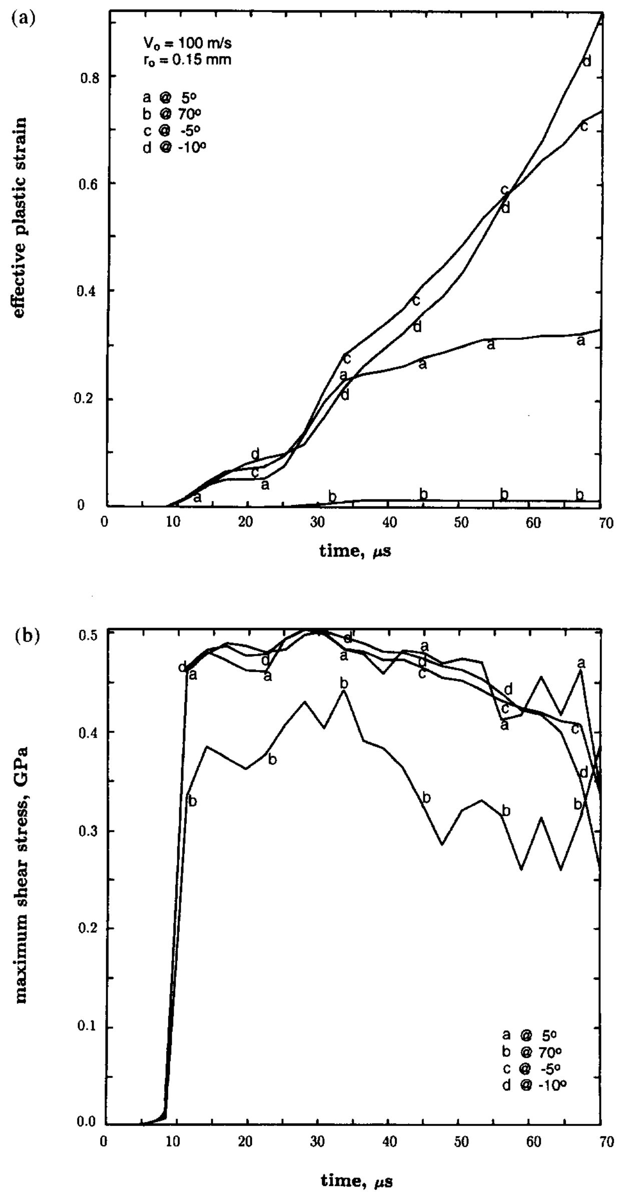

Fig. 7. Time histories of effective plastic strain and maximum shear stress (GPa) at four points adjacent to the notch tip on lines making an angle of (a) 5°, (b) 70°, (c) −5° and (d) −10° to the notch axis for an impact speed of $100\,m\,s^{-1}$ and notch tip radius = 0.15 mm.

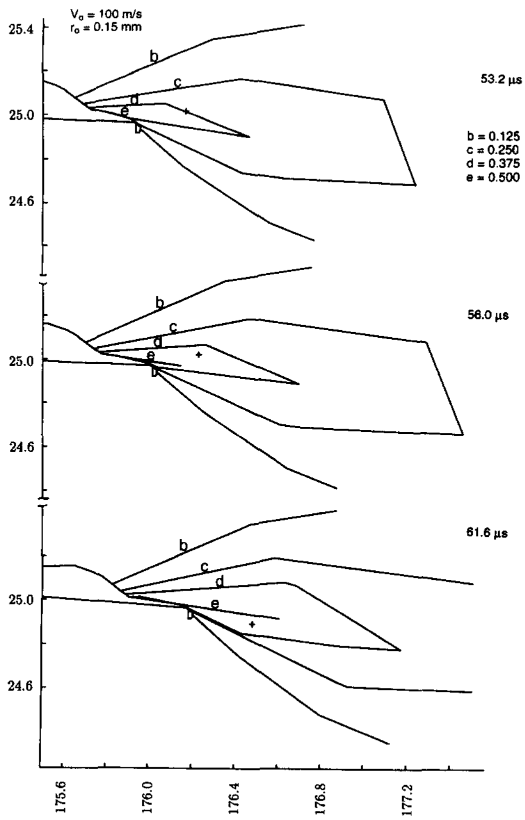

(a)

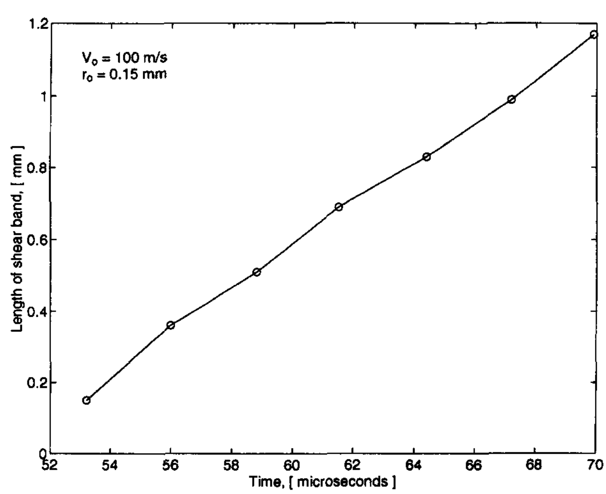

(b)

Fig. 8. (a) Deformed notch tip and contours of the effective plastic strain. Impact speed = $100\,\mathrm{m\,s^{-1}}$, notch tip radius = 0.15 mm. (b) Time history of maximum distance from the notch tip to a point with minimum effective plastic strain of 0.5.

approximately 0.92 mm owing to deformations of the material on the traction free surface of the notch but mostly owing to the rigid body motion of the plate. The contours of the effective plastic strain evince that the deformation has localized in a direction approximately $-5°$ to the notch ligament. We recall that no failure criterion is included in our work. We regard the region with effective plastic strain exceeding 0.50 as the region occupied by a shear band and have plotted in Fig. 8(b) the distance of the farthest point in this region from the notch tip versus time. The slope of this curve equals the speed of a shear band, and the average speed so computed equals $67\,\mathrm{m\,s^{-1}}$. For a single notched speciment of C-300 steel, Zhou *et al.* (1996*a*) found the speed of a shear band to vary from $80\,\mathrm{m\,s^{-1}}$ to $1200\,\mathrm{m\,s^{-1}}$ during the course of its propagation from the notch tip. We note that Batra and Zhang (1994) studied thermomechanical deformations of a 4340 steel thin tube fixed at one end and twisted at the other end by applying a tangential velocity. They found that for a nominal strain rate of $1000\,\mathrm{s^{-1}}$, the contour of shear strain of 2 initiating from a defect at the middle of the tube, propagated circumferentially in both directions at a speed of $40\,\mathrm{m\,s^{-1}}$ at the instant of initiation, to $260\,\mathrm{m\,s^{-1}}$ when it almost reached the diametrically opposite point. Batra and Peng (1996) studied the development of shear bands during the perforation of a 4340 steel plate, and estimated the average speed of a shear band to be about $71\,\mathrm{m\,s^{-1}}$. As pointed out by Zhu and Batra (1991), amongst others, the instantaneous speed of a shear band depends on the local strain, strain rate and temperature.

V. INFLUENCE OF THE NOTCH TIP RADIUS

Keeping the impact speed fixed at $35\,\mathrm{m\,s^{-1}}$, we now vary the notch tip radius. Figure 9 depicts for $r_0 = 0.4$, 0.6 and 0.8 mm the time history of effective plastic strain at points *a*, *b*, *c* and *d* adjacent to the notch surface; their orientations are illustrated in the insert to Fig. 2. These plots suggest that for any fixed value of time, the effective plastic strain at these four points decreases with an increase in the value of the notch tip radius r_0. Also, with an increase in r_0, deformations around the notch tip tend to become uniform. For the four values of r_0 (results for $r_0 = 0.15$ mm and $V_0 = 35\,\mathrm{m\,s^{-1}}$ were discussed in the previous section), the effective plastic strain begins to grow first at point *d* but eventually higher values occur at point *c* for $r_0 = 0.15$, 0.4 and 0.6 mm, and at point *a* for $r_0 = 0.8$ mm. For $r_0 = 0.8$ mm, plastic deformations at $t = 160\,\mu s$ appear to be relatively uniform in the region adjacent to the notch tip. Figure 10(a) shows at $t = 20$, 40 and $60\,\mu s$, the effective plastic strain at points *b* (70°) and *c* ($-5°$) as a function of the notch tip radius r_0. The notch tip radius has very little effect on the plastic deformations at point *b* but significant effect on the plastic deformations at point *c*. However, the effect of the notch tip radius on the maximum tensile hoop stress induced during the time interval $10\,\mu s \leq t \leq 60\,\mu s$ at point *b* is minimal but that at point *d* for $70\,\mu s \leq t \leq 100\,\mu s$ is noticeable as shown in Fig. 10(b). The general nature of the distribution of the hoop stress in the deforming plate region remains unaffected by the value of r_0.

Figure 11(a) depicts the distribution, at $47.6\,\mu s$ after impact, of the maximum shear stress in the plate for $r_0 = 0.4$ mm and $V_0 = 35\,\mathrm{m\,s^{-1}}$. It is clear that the maximum shear stress in a narrow region emanating from the notch tip and ending at the free surface has exceeded 0.4 GPa. The deformed shape of the plate at $47.6\,\mu s$, shown in Fig. 11(b), indicates that it has bent as if bending moments were acting on its top and bottom edges; the deformed shape is plotted with a displacement scale factor of 20 to illustrate its deformations.

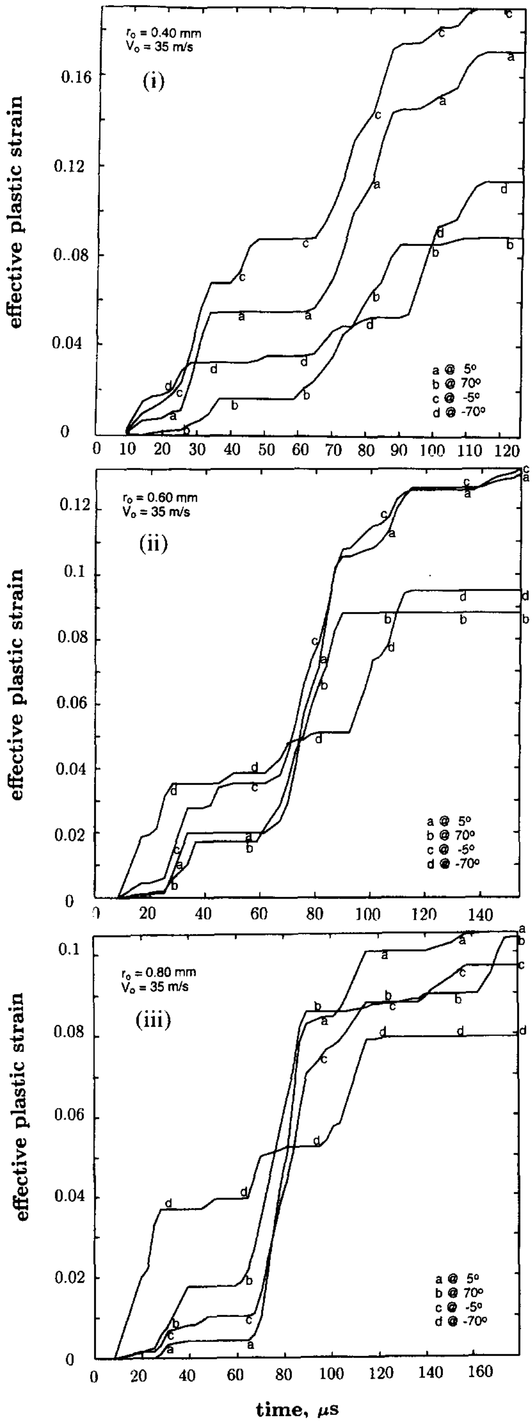

Fig. 9. Time histories of effective plastic strain at four points adjacent to the notch tip; (a) 5°, (b)–5°, (c) –70° and (d) 70°; $V_0 = 35\,\mathrm{ms}^{-1}$. (i) $r_0 = 0.4\,\mathrm{mm}$; (ii) $r_0 = 0.6\,\mathrm{mm}$, and (iii) $r_0 = 0.8\,\mathrm{mm}$.

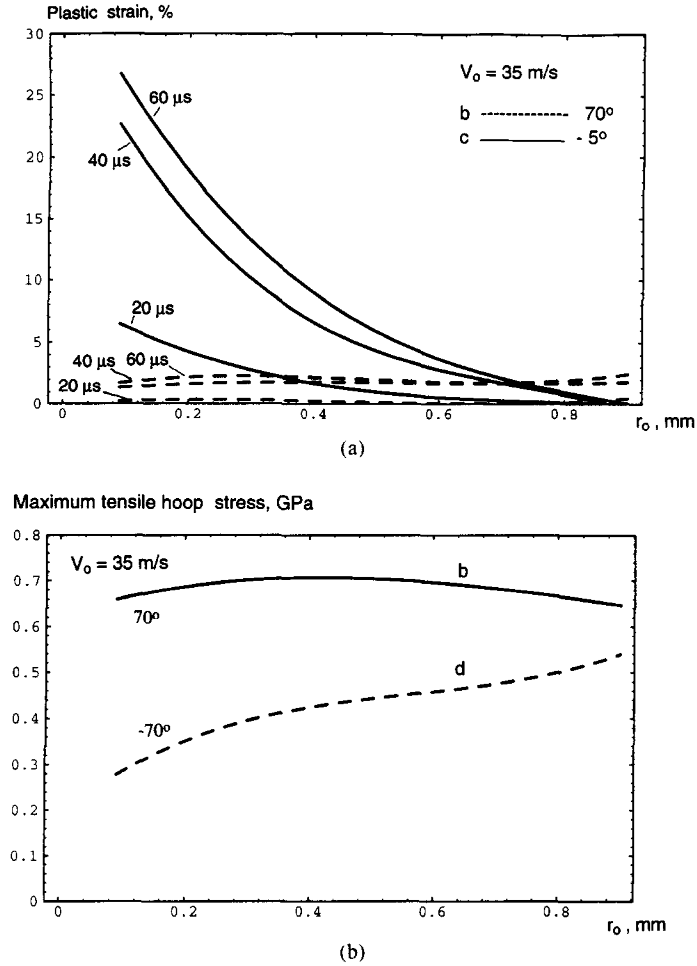

Fig. 10. (a) Effect of the notch tip radius, r_0, on effective plastic strain at two points adjacent to the notch tip in the directions of 70° and −5° to the notch ligament. (b) Effect of the notch tip radius, r_0, on the maximum tensile hoop stress at point b (70°) during $0\,\mu s \leq t \leq 60\,\mu s$, and point d (−70°) during $70\,\mu s \leq t \leq 100\,\mu s$ for impact speed = 35 m s^{-1}.

VI. EFFECT OF MATERIAL'S YIELD STRESS

One of the main differences between the C-300 steel tested by Zhou *et al.* (1996*a*) and the 4340 steel is that the initial yield strength (value of parameter A in the Johnson–Cook model) for the C-300 steel is much higher than that for the 4340 steel. In order to delineate its effect, we increased the value of A from 792 to 2000 MPa, and kept values of remaining parameters in the Johnson–Cook model for both the projectile and the pre-notched plate unaltered. Figure 12 illustrates the evolution of effective plastic strain and maximum shear stress at four points a, b, c and d (cf. the insert to Fig. 2) on the notch surface for $V_0 = 100$ m s^{-1} and $r_0 = 0.15$ mm. A comparison of these results with those in Fig. 7 reveals that effective plastic strains induced are much higher in the steel with $A = 2000$ MPa as compared with those in the steel with $A = 792$ MPa. The drop in the maximum shear stress at points a, c and d indicates that a shear band initiates at $-5°$ to $-10°$ to the notch ligament soon after the initial loading wave arrives at the notch tip at $t = 10\,\mu$s. The shear band initiates also at 5° to the notch ligament at $t = 28\,\mu$s. The evolution of the effective plastic strain suggests that the shear band at point d is dominant as it has the maximum effective plastic strain among the bands at points a, c and d. Since it is highly unlikely that a material point will sustain plastic strains of 200% without fracture, a shear crack will initiate at point d, i.e. in the direction of $-10°$ to the notch ligament. The initiation of a crack results in the formation of new free surfaces and changes the boundaries of the domain analysed.

VII. CONCLUSIONS

We have analysed plane strain thermomechanical deformations of a pre-notched 4340 steel plate impacted at the notched surface by a 4340 steel projectile. The material is modeled by the Johnson–Cook relation that accounts for its strain hardening, strain-rate hardening, and thermal softening. The effect of impact speed, notch tip radius and the quasistatic yield stress of the material on deformations of the material in the notch-tip vicinity has been delineated. With an increase in the impact speed, effective plastic strains grow faster at points situated adjacent to the notch-tip surface and making an angle of 5° to $-10°$ to the notch ligament. The growth rate of effective plastic strain at points in the 70° and $-70°$ directions is essentially unaffected by the impact speed. The plastic strain localization may result in shear cracking within a zone of maximum shear and compressive

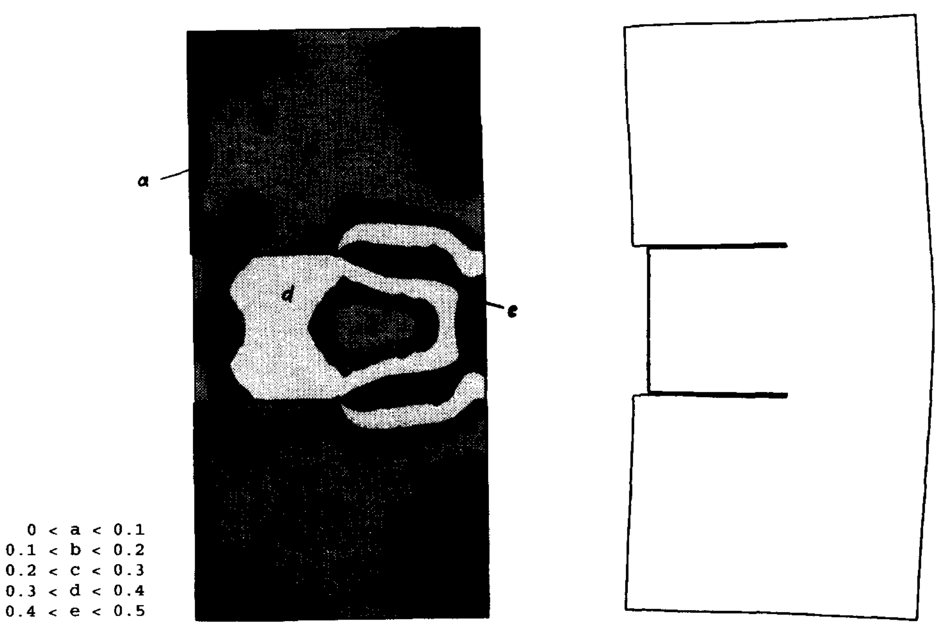

(a) (b)

Fig. 11. Distribution of maximum shear stress (GPa) and deformed shape of the double notch plate (displacement scale factor = 20) at 47.6 μs. Impact speed = 35 m s^{-1}, notch tip radius = 0.4 mm.

hoop stresses at points in an angular sector of 0° to −10° to the notch ligament. The maximum tensile hoop stress occurs at points on the notch surface in the 70° direction and may result in an opening crack; these values are essentially unaffected by the notch tip radius. However, at points on the notch-tip surface in the −70° direction, the tensile hoop stress grows with an increase in the notch tip radius r_0. Also, for large values of r_0, the plastic deformations are uniformly distributed around the notch tip. An increase in the quasistatic yield stress of the material results in much higher plastic strains at points on the notch-tip surface with a shear band initiating first at a point in the −10° direction to the notch ligament.

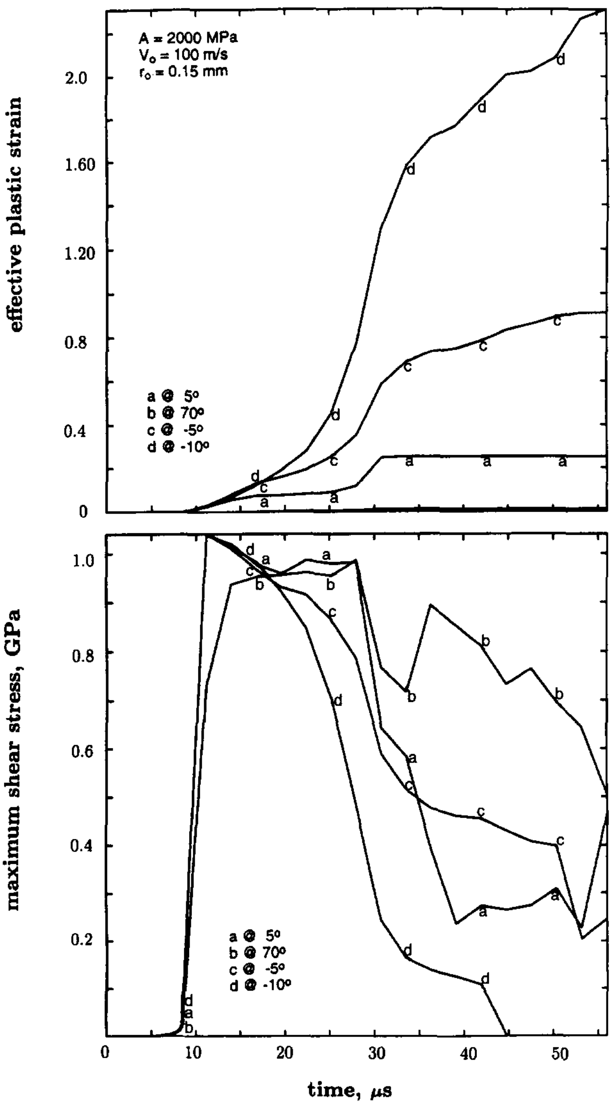

Fig. 12. Time history of effective plastic strain and maximum shear stress (GPa) at four points on the notch surface for impact speed = 100 m s^{-1}, notch tip radius = 0.5 mm, and material parameter A = 2000 MPa.

Acknowledgements—The support of this work from the Office of Naval Research under grant number N00014-94-1-1211 with Dr Y.D.S. Rajapakse as the program manager is gratefully acknowledged.

REFERENCES

Batra, R. C. and Hwang, J. (1994) Dynamic shear band development in dipolar thermoviscoplastic materials. *Comp. Mechs.* **14**, 354.

Batra, R. C. and Peng, Z. (1996) Development of shear bands during the perforation of a steel plate. *Comp. Mechs.* **17**, 326.

Batra, R. C. and Zhang, X. T. (1994) On the propagation of a shear band in a steel tube. *J. Engng. Mater. Tech.* **116**, 155.

Farren, W. S. and Taylor, G. I. (1925) The heat developed during plastic extrusion of metal. *Proc. R. Soc.* **A207**, 422.

Johnson, G. R. and Cook, W. H. (1983) A constitutive model and data for metals subjected to large strains, high strain rates, and high temperatures. *Proc. 7th Int. Symp. Ballistics,* The Hague, The Netherlands, p. 541.

Kalthoff, J. F. (1987). Shadow optical method of caustics. In *Handbook on Experimental Mechanics*, ed. A. S., Kobayashi, p. 430. Prentice-Hall, Englewood Cliffs, NJ.

Kalthoff, J. F. (1990) Transition in the failure behavior of dynamically shear loaded cracks. *Appl. Mech. Rev.* **43**, S247.

Kalthoff, J. F. and Winkler, S. (1988) Failure mode transition at high strain rates of loading. *Proc. Int. Conf. on Impact Loading and Dynamic Behavior of Materials*, eds C. Y. Chiem, H. D. Kunze and L. W. Meyer, p. 185. Deutsche Gewsellschaft fur Metallkundcle, DGM, Bremen.

Klepaczko, J. R., Lipinski, P. and Molinari, A. (1987) An analysis of the thermoplastic catastrophic shear in some metals. *Proc. Int. Conf. on Impact Loading and Dynamic Behavior of Materials*, eds C. Y. Chiem *et al.*, p. 695. Informations Gesellaschaft Verlag Oberursel.

Marchand, A. and Duffy, J. (1988) An experimental study of the formation process of adiabatic shear bands in a structural steel. *J. Mechs. Phys. Solids* **36**, 251.

Mason, J. J., Rosakis, A. J. and Ravichandran, G. (1994) Full field measurements of the dynamic deformation field around a growing adiabatic shear band at the tip of a dynamically loaded crack or notch. *J. Mechs. Phys. Solids* **42**, 1679.

Nechitailo, N. V. (1995) Finite element analysis of failure modes in dynamically loaded pre-cracked steel plates. M.S. Thesis, Virginia Polytechnic Institute and State University.

Needleman, A. (1988) Material rate dependence and mesh sensitivity in localization problems,. *Comp. Meth. Appl. Mech. Engng* **67**, 69.

Rajendran, A. M. (1992) High strain rate behavior of metals, ceramics and concrete. Report No. WL-TR-92-4006, Wright Patterson Air Force Base.

Ravi-Chandar, K. (1995) On the failure mode transitions in polycarbonate under dynamic mixed-mode loading. *Int. J. Solids and Structures* **32**, 925.

Sulijoadikusumo, A. U. and Dillon, O. W., Jr. (1979) Temperature distribution for steady axisymmetric extrusions with an application to Ti–6Al–4V, Part I. *J. Thermal Stresses* **2**, 97.

Truesdell, C. A. and Noll, W. (1965) Nonlinear Field Theories of Mechanics in *Handbuch der Physik*, ed. S. Flügge. Springer-Verlag, Berlin–Heidelberg–New York.

Whirley, R. G., Englemann, B. E. and Hallquist, J. P. (1992) DYNA2D, A nonlinear, explicit, two-dimensional finite element code for solid mechanics, user manual. Lawrence Livermore National Laboratory Report, UCRL-MA-110630.

Zhou, M., Rosakis, A. J. and Ravichandran, G. (1996*a*) Dynamically prenotched plates. Part I—Experimental investigations of temperature signatures and propagation speed. *J. Mechs. Phys. Solids* **44**, 981.

Zhou, M., Ravichandran, G. and Rosakis, A. J. (1996*b*) Dynamically propagating shear bands in impact-loaded prenotched plates—II, Numerical simulation. *J. Mechs. Phys. Solids* **44**, 1007.

Zhu, Z. G. and Batra, R. C. (1991) Shear band development in a thermally softening viscoplastic body. *Computer Structures* **39**, 459.